Desalination and Water Treatment
www.deswater.com

doi: 10.1080/19443994.2014.979239

57 (2016) 388–397
January

Taylor & Francis
Taylor & Francis Group

Adsorptive removal of sulfa antibiotics from water using spent mushroom substrate, an agricultural waste

Aixia Zhou[a,b], Yuling Zhang[a,b,*], Rui Li[a,b], Xiaosi Su[a,b], Lanying Zhang[a]

[a]*Key Laboratory of Groundwater Resources and Environment, Ministry of Education, Jilin University, Changchun, China, Tel. +86 15144148018; emails: zhouaixia2010@sina.com (A. Zhou), lingling29@126.com (Y. Zhang), 895605812@qq.com (R. Li), 335893987@qq.com (X. Su), 1103780978@qq.com (L. Zhang)*
[b]*Institute of Water Resources and Environment, Jilin University, Changchun, China*

Received 22 March 2014; Accepted 15 October 2014

ABSTRACT

The potential for spent mushroom substrates (SMS) to remove sulfa antibiotics (sulfas) from water was evaluated in a batch process. Experiments were carried out as a function of contact time, initial concentration (0.5–10 mgL^{-1}), and pH (1–11). Adsorption isotherms were modeled using the Langmuir and Freundlich models. The data fit the Langmuir isotherm well. The maximum adsorption capacities were found to be 2.1072, 1.8103, 2.2991, and 2.2133 mg g^{-1} at 288 K for sulfamethyldiazine, sulfamethazine, sulfathiazole, and sulfamethoxazole, respectively. The kinetic data were analyzed using pseudo-first-order, pseudo-second-order, and intra-particle models. The results indicated that SMS could be an alternative to more costly adsorbents used for removal of trace sulfas.

Keywords: Adsorptive removal; Sulfa antibiotics; Spent mushroom substrate; Agricultural waste

1. Introduction

Sulfonamide antibiotics (sulfas) comprise a class of synthetic, primarily bacteriostatic, sulfanilamide derivatives that are used in human therapy, livestock production, and aquaculture. Treated individuals excrete a fraction of the administered dose as the unaltered parent compound or an acetylated metabolite [1] susceptible to reactivation by bacterial deacetylation [2,3]. Sulfonamides enter the environment through disposal of domestic and hospital waste and via runoff and infiltration from confined animal feeding operations and fields treated with animal manure.

Sulfas rank among the most frequently detected pharmaceuticals in streams in the United States and have been found in groundwater, landfill leachate, and runoff from soils beneath effluent-irrigated lands [4–7]. Antibiotics have also been detected in Chinese surface water, with sulfa concentrations of 0–775 ng L^{-1}[8]. Antibiotics are usually detected in the higher mg L^{-1} range in hospital effluent, lower mg L^{-1} range in municipal wastewater, and at ng L^{-1} levels in surface, sea, and groundwater [9–12]. Although the trace concentrations of sulfas found in aquatic environments do not exceed any current water standards, the extensive use of these antibiotics could result in an increase in bacterial resistance to these antibiotics [13–16]. There have also been warnings of their potential to harm human health [17,18].

---

*Corresponding author.

Spent mushroom substrate (SMS), which is a readily available agricultural waste, has been investigated for its potential to remove organic contaminants from water [19,20]. However, there have been no reports of the use of SMS for the adsorptive removal of antibiotics, including sulfa antibiotics. SMS is a complex organic material that remains after mushrooms have been harvested. The use of SMS as a sorbent would also contribute to its revaluation and help resolve environmental problems caused by its accumulation in landfills. For each ton of mushrooms produced, at least five times the amount of SMS is generated, all of which must be disposed of [21,22].

This study was conducted to evaluate the feasibility of using SMS as a low-cost alternative adsorbent for the removal of trace concentrations of sulfas from water. The effects of initial antibiotics concentration, initial pH, and contact time on sulfas adsorption onto SMS were investigated. Isotherms and kinetics of the adsorption process were also evaluated.

2. Materials and methods

2.1. Adsorbates

The sulfas were supplied by Sigma (St. Louis, MO USA). Four sulfas were used as adsorbates (Table 1).

Standard stock solution of 5 g L^{-1} sulfas in methanol was prepared. During preparation of the SM (sulfamethyldiazine) stock solution, a couple drops of NaOH solution were added to promote its dissolution. The standard solutions were stored at −20˚C until further use.

2.2. Chromatographic analyses

The concentrations of the four sulfas were determined by HPLC–UV using an Agilent 1200 LC (Santa Clara, CA, USA) equipped with an Agilent Intelligent UV detector (270 nm), and a 4.60 × 150 mm, 5-μm XDB C18 analytical column (Agilent). The analytical column was kept at 30˚C and eluted with 0.1% formic acid solution: methanol (70:30 by volume) at a flow rate of 0.8 mL min^{-1}. Under these conditions, the retention times for ST, SM, SM2, and SMX were 3.028, 3.888, 5.151, and 7.158 min, respectively, and the injection volume was 50 μL. All solvents were of chromatographic grade and were filtered through a 0.22-μm membrane prior to use.

2.3. Preparation and characterization of SMS adsorbent

SMS used in this study was obtained from the mushroom shed in Changchun, China. The sample was soaked in distilled water for 24 h, then washed, filtered, and dried in an oven at 35˚C for 4 h. The dried materials were subsequently sieved to the desired mesh size (100–300 μm), after which the prepared SMS samples were stored in an airtight container until further use. The composition of the SMS is listed in Table 2.

Table 1
Properties and characteristics of four sulfa antibiotics [23,24]

Adsorbate	Sulfamethyldiazine (SM)	Sulfamethazine (SM2)	Sulfathiazole (ST)	Sulfamethoxazole (SMX)
Chemical structure	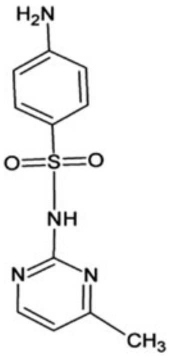	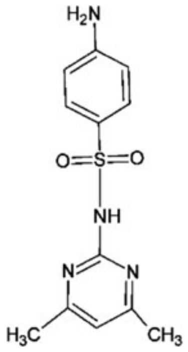	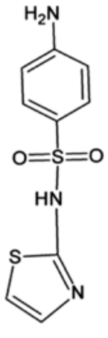	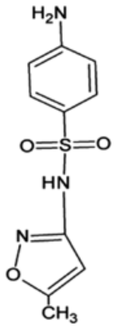
Chemical formula	$C_{11}H_{12}N_4O_2S$	$C_{12}H_{14}N_4O_2S$	$C_9H_9O_2N_3S_2$	$C_{10}H_{11}N_3O_3S$
Formula weight (g mol^{-1})	264.30	278.32	255.3	253.28
Density (g cm^{-3})	1.439	1.391	1.696	1.08
p$K_{a,1}$	2.06	2.3	2.0	1.8
p$K_{a,2}$	6.09	7.49	7.11	5.6
Mv (cm^3 mol^{-1})	183.5	199.8	163.5	173.1
Water solubility (g L^{-1})	0.15	0.485	1.558	1.725

Table 2
Composition of SMS [25]

Ingredient	Protein	Cellulose	Crude fat	Ash	Water	TOC
Content (wt %)	12.89	18.45	2.85	6.45	11.78	30.21

The functional groups available on the surface of the prepared SMS before and after sulfa antibiotic adsorption were detected by the KBr technique using a Fourier transform infrared (FTIR) spectroscope (FTIR-2000, PerkinElmer, Waltham, MAU, USA). The KBr pellets were obtained by uniformly pressing 1 mg prepared samples and 300 mg of KBr under vacuum. The spectra were recorded from 4,000 to 400 cm^{-1}, and the surface morphology of the porosity of the SMS was studied using scanning electron microscopy (SEM) analysis.

2.4. Batch equilibrium and kinetic studies

Adsorption experiments were carried out by adding a fixed amount of SMS (0.10 g) to a series of 250-mL conical flasks filled with 50-mL diluted solutions (0.5–10 mg L^{-1}). The conical flasks were then sealed and shaken at 100 rpm for the required time. Next, the solution was centrifuged at 5,000 rpm and 1 mL of supernatant was filtered through a 0.22-μm fibrous membrane and analyzed by HPLC–UV. The amount of antibiotics adsorption at equilibrium q_e (mg g^{-1}) was calculated from the following equation:

$$q_e = \frac{(C_0 - C_e)V}{W} \tag{1}$$

where q_e (mg g^{-1}) is the adsorption capacity of antibiotics at equilibrium, C_0 and C_e (mg L^{-1}) are the initial concentration and equilibrium concentration of antibiotics, respectively, W is the adsorbent mass, and V is the volume of the adsorption system.

The initial concentration was set to 0.5, 1, 2, 5, or 10 mg L^{-1}, while the initial pH was set at 1, 3, 5, 7, 9, or 11 to investigate the effects of these factors on the adsorption capacity of SMS. All experiments were replicated three times.

3. Results and Discussion

3.1. Characteristics of SMS

The FTIR spectra of raw SMS before and after sulfas were adsorbed from an initial concentration of 5 mg L^{-1} were basically the same, with only minute peaks at 450, 515, 780, 1,180, 1,250, and 1,633 cm^{-1} appearing after sulfas adsorption onto SMS owing to the lower amount of sulfas uptake. The infrared spectrum revealed the principal surface functionalities of raw SMS (Fig. 1). The spectrum of SMS was characterized by five bands, 3,380, 2,930, 1,400, 1,060 and 1,580 cm^{-1}, which were attributed to hydroxyl groups (–OH), C–H stretching vibrations, C=O stretching vibrations, 1,4-glycosidic bonds, aromatic C=C rings or COO– group stretching, respectively [26–31].

The –NH$_2$ vibration absorption peaks at 3,424 and 3,354 cm^{-1} with N–H stretching of sulfonamide at 3,269 cm^{-1} [32]. The stretching frequency of the N–H of the sulfas has been reported to be 3,379 cm^{-1}, while the calculated and experimental in-plane N–H mode was at 1,499 and 1,454 cm^{-1}, respectively [33]. A new band appeared at 1,633 cm^{-1}, which was probably owing to the bending mode of the sulfas-NH$_2$ group [34]. In this study, a weak band remained at 1,652 cm^{-1}, which could have been owing to N–H$_3^+$ bending of sulfas rather than the bending mode of the sulfa–NH$_2$ group.

Vibrations at 1,324 and 1,150 cm^{-1} were attributed to symmetric and asymmetric vibration absorption peaks of -SO$_2$- [34]. The bands at 1,150 and 1,092 cm^{-1} were assigned to symmetric SO$_2$ N and substituted benzene rings [35]. After sulfas adsorption onto SMS, two smaller peaks were observed at 831 and 791 cm^{-1} as a result of –OH and aliphatic CH$_2$ deformation [32]. Additionally, a band was observed at 637 cm^{-1} due to the N–H vibration produced by adsorptions between the N of the sulfas and the substituted benzene ring with the surface of SMS. Similarly, interactions between sulfas and high silica zeolite Y were found

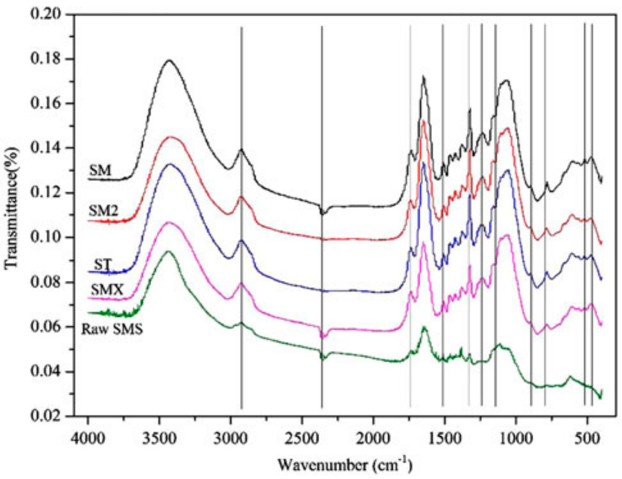

Fig. 1. FTIR spectra of SMS before and after adsorption of the four sulfa antibiotics.

to involve multiple weak H-bonds and van der Waals type interactions between the amine protons of sulfas and lattice oxygen atoms and hydrophobic interactions between the aromatic rings and zeolite cage walls [33].The weak peak at 2,350 cm^{-1} was probably due to the ammonium vibration or amino acid hydrochloride.

SEM images (20,000 × magnification) of the dry absorbents with different dispositions shown in Fig. 2(A) depict the sagging structure on the surface. As shown in Fig. 2(B), after adsorption with antibiotics, the surface of SMS had a floccule-like membrane and a blurred outline. These characteristics may be owing to macromolecular sulfas adsorbed onto the surface.

3.2. Effects of antibiotics concentration and contact time

Fig. 3 shows the adsorption capacity vs. the initial antibiotics concentrations at 288 K. The sulfas adsorption capacity increased as the initial antibiotics concentration increased. Specifically, the adsorption capacity (q_e) of the sulfas equilibrium increased from 0.710 to 2.299 $\mathrm{mg\,g}^{-1}$ as the sulfas concentration increased from 0.5 to 10 $\mathrm{mg\,L}^{-1}$. The initial antibiotics concentration provided the necessary driving force to overcome resistance to the mass transfer of sulfas between the aqueous and solid phases.

The adsorption of sulfas onto SMS was also studied as a function of contact time to determine the equilibrium time for maximum adsorption. The results showed that the equilibrium time required for the adsorption of sulfas onto SMS had a range of 150–180 min (Fig. 4). Based on these results, 180 min was fixed as the equilibrium time for the remainder of the study.

3.3. Competitive adsorption

The adsorption capacity of sulfas differs owing to differences in the chemical structures and functional groups. As shown in Fig. 4, the adsorption capacity of the four sulfas onto SMS occurred in the order: ST > SMX > SM > SM2. This was because the N-hetero-aromatic ring of ST has no methyl functional groups, decreasing the stereo hindrance, which makes the hydrogen bonds formed between the N-hetero-aromatic ring and SMS surface strong, enhancing adsorption capacity. The molecular volume of ST was smallest among the investigated sulfas, so it can more easily enter a molecular sieve orbit, resulting in high adsorption capacity. The molecular weight and molecular volume of SM2 are larger than those of the other three sulfas, and the N-hetero-aromatic ring of SM2 has two methyl functional groups; therefore, the adsorption capacity of SM2 is smallest.

3.4. Adsorption mechanism

Fig. 5 shows the adsorption capacity for sulfas onto SMS at different pH. The adsorption capacity of the four sulfas onto SMS decreased from around 2.4 to around 1 $\mathrm{mg\,g}^{-1}$ as the pH of the initial solution increased from 1 to 11, gradually becoming constant as the pH became neutral and more basic. As shown in Table 1, because the pK_a values of sulfas have a range of 5.6–7.49 and 1.8–2.3, the deprotonated

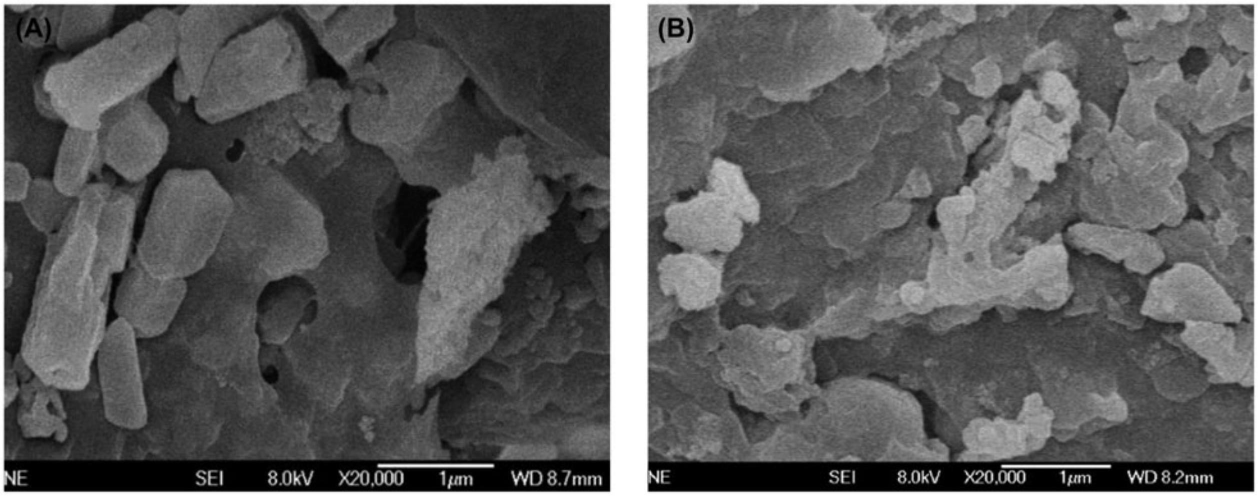

Fig. 2. SEM micrograph of SMS sample before and after antibiotics adsorption: (A) before adsorption and (B) after adsorption of four sulfa antibiotics.

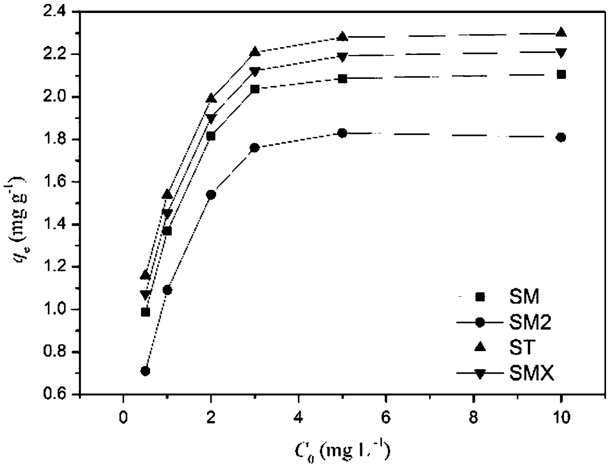

Fig. 3. Effects of initial antibiotics concentration on the adsorption of sulfas onto SMS.

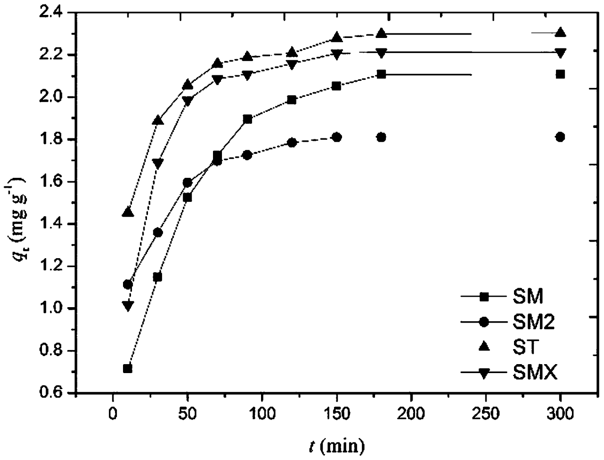

Fig. 4. Effects of contact time on adsorption uptake of sulfas onto SMS.

(anionic) form of sulfas is prevalent at alkaline pH, but cationic and non-ionized sulfas would be dominant at neutral and lower pH. All sulfas showed the highest adsorption onto SMS at 1–3. Overall, the anionic form of sulfas appeared to adsorb less than the cationic and non-ionized form. These findings are similar to the results of previous studies [36].

It is likely that hydrophobic partitioning with organic matter will be dominant at pH 1–3 owing to the strong electrostatic attraction between cationic sulfas and negative forces. At pH 3–7, the non-ionized form of sulfas is dominant and the adsorption is mainly due to the hydrogen bond. As the pH increases, the cationic form decreases and the adsorption capacity decreases. At high pH, the anionic sulfas result in significantly less hydrophobic partitioning than the non-ionized form of sulfas, and the electrostatic repulsion between anionic sulfas and the negatively charged SMS surface may increase accordingly. Therefore, the lower sorption at high pH may be attributed to the anionic sulfas, where hydrophobic sorption would be impacted by the electrostatic repulsion of the anionic sulfas and the negative charge of SMS at high pH [37]. Consequently, the high adsorption capacity of sulfas on SMS occurs at low pH. It is worth noting that a significant amount of sulfas removal onto SMS was observed as the pH of the solution increased from 7 to 11. These findings suggest that a mechanism other than electrostatic attraction may be operating [38].

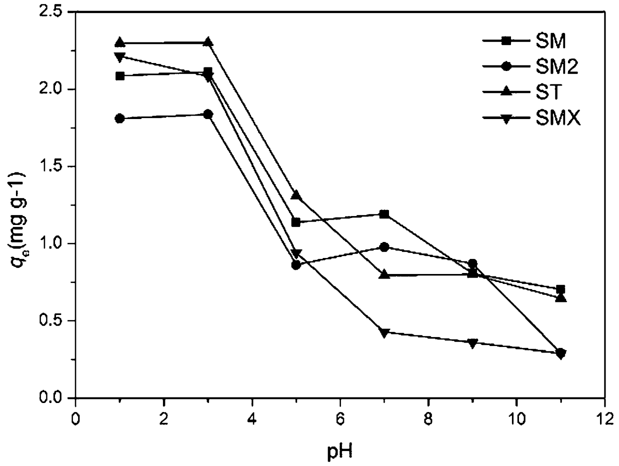

Fig. 5. Effect of pH on the adsorption of sulfas onto SMS.

3.5. Adsorption kinetics studies

To examine the mechanism controlling adsorption processes such as mass transfer and chemical reaction, pseudo-first-order, pseudo-second-order, and intraparticle diffusion kinetic equations were used to fit the experimental kinetic data.

The mathematical forms of the pseudo-first-order model [39] and the pseudo-second-order model [39] are shown in Eqs. (2) and (3):

$$\log(q_e - q_t) = \log q_e - \left(\frac{k_1}{2.303}\right)t \tag{2}$$

$$\frac{t}{q_t} = \frac{1}{k_2 q_e^2} + \frac{t}{q_e} \tag{3}$$

where q_e and q_t (mg g^{-1}) are the adsorption capacity of antibiotics at equilibrium and at time t (min), respectively, and k_1 (min^{-1}) and k_2 (min^{-1}) are the rate constant of pseudo-first adsorption and pseudo-second adsorption, respectively. The linear plots of log ($q_e - q_t$) vs. t and t/q_t against t are shown in Fig. 6(a) and (b), respectively. The values of k_1, k_2, and q_e calculated from the plots are presented in Table 3. As shown in the table, the adsorption data were well represented by the pseudo-second-adsorption model, with an $r^2 > 0.99$ for all four sulfas. The calculated q_e ($q_{e,\ cal.}$) value obtained in the pseudo-second-adsorption model agreed with the experimental values of q_e ($q_{e,\ exp}$), indicating the experimental data are better described by the pseudo-second-adsorption model than the pseudo-first-adsorption model. These results showed that the rate-limiting step may be the adsorption mechanism.

The intra-particle diffusion model [40] proposed by Weber and Morris was used to investigate the intra-particle diffusion mechanism:

$$q_t = k_i t^{1/2} + C \tag{4}$$

where k_i (mg g min$^{-1/2}$) is the intra-particle diffusion rate constant and C is a constant that gives information about the thickness of the boundary layer. In this model, a larger intercept is associated with a greater boundary layer effect. The plot of q_t vs. $t^{1/2}$ is presented in Fig. 6(c). The values of the intra-particle diffusion kinetics model parameters, k_i and C, were obtained from the slope and intercept of the plot, respectively, and are listed in Table 3. If the regression of qt vs. $t^{1/2}$ is linear and passes through the origin, intra-particle diffusion is the sole rate-limiting step. As shown in Fig. 6(c), the value of q_t initially increases rapidly, then increases at a lesser rate, indicating that the adsorption of sulfas on SMS is a multi-step process consisting of adsorption onto the external surface, diffusion into the interior, and a final equilibrium stage. The adsorption process can be divided into two steps that are ascribed to the intra-particle diffusion stage and the equilibrium stage because the step of adsorption onto the external surface is rapid and less

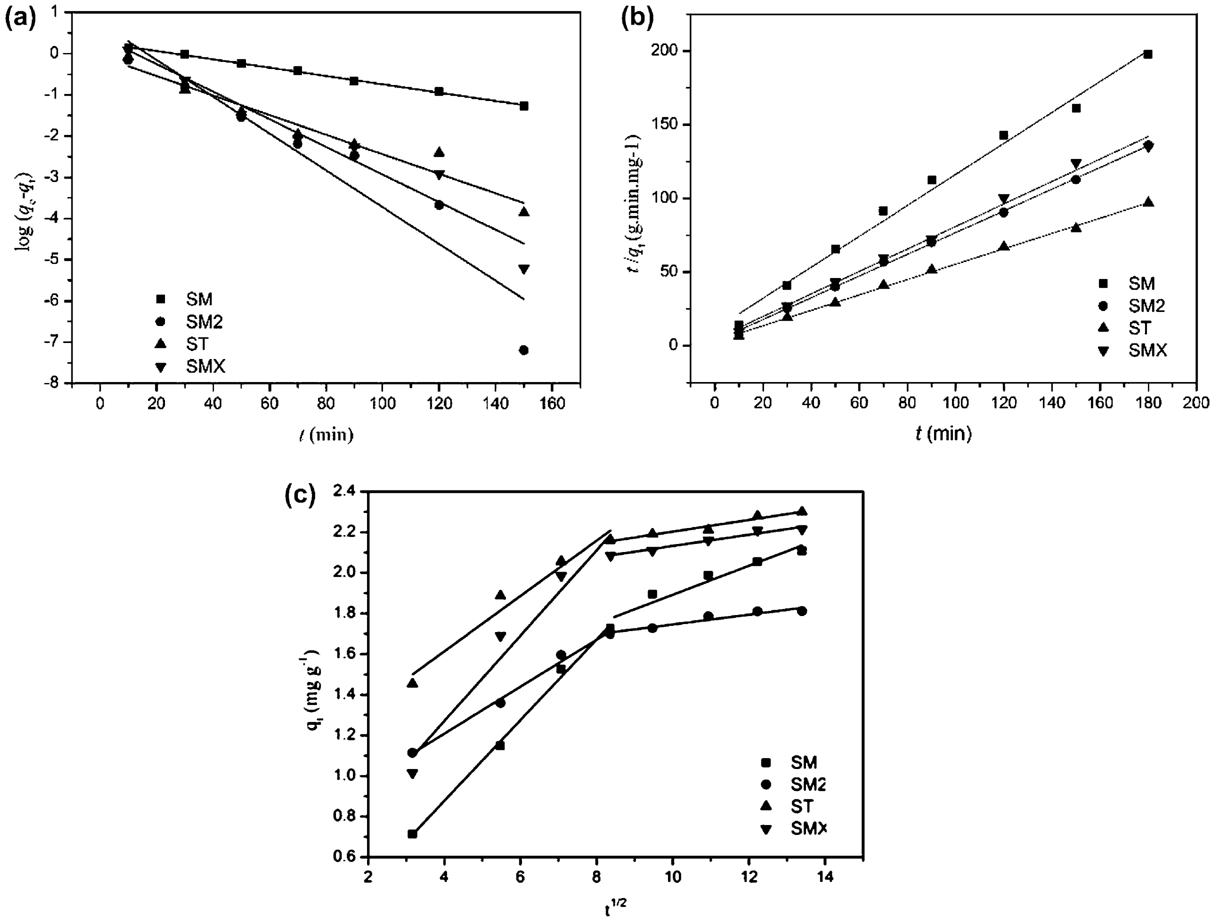

Fig. 6. Linear plots of the (a) pseudo-first-order kinetics, (b) pseudo-second-order kinetics, and (c) intra-particle diffusion kinetics model for adsorption of sulfas onto SMS at 288 K.

Table 3
Kinetic parameters for the removal of antibiotics by SMS

Kinetic models	SM	SM2	ST	SMX
$q_{e,exp}$ (mg g-1)	2.107	1.81	2.299	2.213
Pseudo-first-order				
k_1 (× 10^{-2} min^{-1})	2.328	10.285	5.463	7.717
r^2	0.9973	0.8777	0.9375	0.9302
$q_{e,cal}$ (mg g^{-1})	1.852 ± 0.01	5.522 ± 0.012	0.856 ± 0.009	2.618 ± 0.011
Pseudo-second-order				
k_2 (g mg^{-1} min^{-1})	0.208	0.388	0.749	0.495
r^2	0.9973	0.9993	0.9997	0.9994
$q_{e,cal}$ (mg g^{-1})	2.45 ± 0.010	1.913 ± 0.008	2.384 ± 0.006	2.368 ± 0.007
Intra-particle diffusion				
k_{i1} (mg g^{-1} $\text{min}^{-1/2}$)	0.19869	0.11572	0.13619	0.21016
C_1	0.08246	0.74528	1.06872	0.42929
r^2	0.99405	0.98743	0.94624	0.92818
k_{i2} (mg g^{-1} $\text{min}^{-1/2}$)	0.07142	0.02413	0.02883	0.02764
C_2	1.17539	1.50283	1.91256	1.85386
r^2	0.91923	0.89948	0.94837	0.95653

obvious. Because the first linear plot corresponding to the intra-particle diffusion stage does not cross the origin, some degree of boundary layer control exists, which further shows that intra-particle diffusion is not the only rate-controlling step and that other processes may control the rate of adsorption.

3.6. Adsorption isotherms

The adsorption isotherms indicate the distribution of adsorbed molecules between the liquid phase and the solid phase when the adsorption process reaches an equilibrium state. Adsorption isotherms are important for the description of how molecules of the adsorbate interact with the adsorbent surface. Hence, the adsorption of sulfas onto SMS is determined as a function of equilibrium sulfas concentration (C_e), and the corresponding adsorption isotherm is plotted in Fig. 7(a) and (b). According to the classification by Giles et al. [41], the isotherm appears to be of the L type, indicating that the isotherm is connected with the flat position of the adsorbate molecule toward the adsorbent surface and there is monolayer coverage.

The isotherm data were fitted to the Langmuir and Freundlich isotherms in Fig. 7(a) and (b), respectively

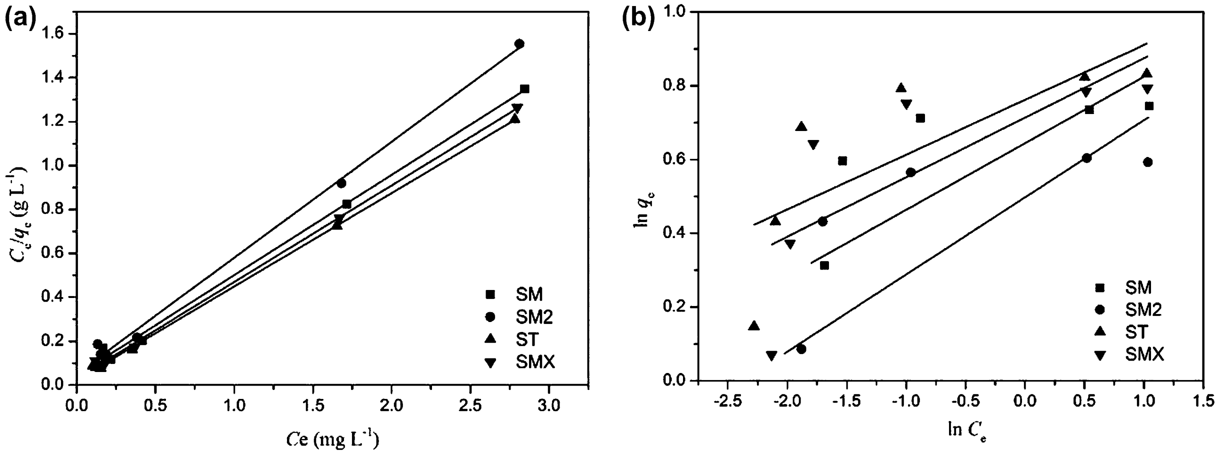

Fig. 7. Equilibria for sulfa antibiotics adsorption onto SMS: (a) Langmuir plots of the isotherms and (b) Freundlich plots of the isotherms.

[42,43], which are represented by the following equations:

$$\frac{C_e}{q_e} = \frac{C_e}{q_m} + \frac{1}{bq_m} \tag{5}$$

$$\log q_e = \ln K_F + \frac{1}{n} \log C_e \tag{6}$$

where C_e is the equilibrium concentration (mg L^{-1}), q_e is the equilibrium capacity of sulfas on SMS (mg g^{-1}), q_m is the monolayer adsorption capacity of the adsorbent (mg g^{-1}), and b is the Langmuir constant (L mg^{-1}), relate to adsorption capacity and rate of adsorption. The parameters b and q_m were calculated from the intercept and slope, respectively (Table 4). K_F and n (dimensionless) are Freundlich constants, with n indicating how favorable the adsorption process is and K_F indicating the adsorption capacity of the adsorbent. n and K_F can be calculated from the slope and intercept of the plot, respectively (Table 4).

Comparison of the correlation coefficients, r^2, indicated that the experimental equilibrium adsorption data were better described by the Langmuir equation than the Freundlich model. These findings suggest monolayer coverage of the surface of SMS by sulfas.

The essential characteristics of the Langmuir isotherm can be expressed by a dimensionless constant known as the equilibrium parameter, R_L [44–46]:

$$R_L = \frac{1}{1 + bC_0} \tag{7}$$

where b is the Langmuir constant and C_0 (mg L^{-1}) is the initial antibiotics concentration. The value of R_L indicates the type of the isotherm to be either unfavorable ($R_L > 1$), linear ($R_L = 1$), favorable ($0 < R_L < 1$), or irreversible ($R_L = 0$). Values of R_L were found to vary between 0 and 1, which confirmed that the SMS is favorable for adsorption of sulfas under the conditions investigated.

As shown in Table 5, the adsorption effect of SMS is much better than that of other commonly used

Table 4
Langmuir and Freundlich parameters for antibiotic adsorption

	Langmuir equation				Freundlich equation		
Antibiotics	q_0 (mg g^{-1})	b (L mg^{-1})	R_L	r^2	K_F ($mol^{1-1/n}$ $L^{1/n}$ g^{-1})	n	r^2
SM	2.45	0.266	0.0075	0.99625	1.905	5.542	0.803
SM2	1.913	10.144	0.0193	0.99483	1.645	4.78	0.840
ST	2.384	18.072	0.0109	0.9991	2.143	6.731	0.847
SMX	2.368	14.750	0.0134	0.99851	2.718	6.197	0.846

Table 5
Comparison with other adsorbents of sulfa antibiotics

Adsorbent	Antibiotics	Adsorption capacity (mg g^{-1})	T (K)	Initial concentration (mg L^{-1})
Activated carbons [47] modified by oxidation	Sulfadiazine	1.67	303	20
	Sulfamethoxydiazine	1.67	303	20
	Sulfamethazine	1.67	303	20
	Sulfaquinoxaline	1.67	303	20
Magnetic nano-composite CoFeM48 [48]	Sulfathiazole (STZ)	0.0987	288	100
	Sulfamethazine (SMN)	0.068	288	100
	Sulfamethizole (SML)	0.099	288	100
	Sulfamethoxazole (SMX)	0.0824	288	100
	Sulfadimethoxine (SDM)	0.099	288	100
Fly ash [49]	Sulfonamide	0.06–0.18	298	50
SMS	SM	2.45	288	10
	SM2	1.913	288	10
	ST	2.384	288	10
	SMX	2.368	288	10

adsorbents. In addition, SMS is an environmentally friendly material that is easily biodegraded and has rarely been reported to cause secondary pollution. SMS effectively removed sulfas from the water at 288 K, indicating that it can be used for groundwater or other low-temperature water applications. In terms of costs, SMS is less expensive than activated carbons and other synthetic materials. In conclusion, SMS is an effective, inexpensive, and environmentally friendly adsorbent that can be used for removal of sulfa antibiotics.

4. Conclusions

This study investigated the ability of SMS to remove sulfas from aqueous solution and described the characteristics of SM, SM2, SMX, and ST sorption onto SMS. The adsorption capacity of SMS increased as the initial concentration increased; however, the adsorption capacity decreased as the pH increased from 3 to 11. The effects of pH suggest that electrostatic attraction was not the only mechanism involved in sulfa antibiotics adsorption in the present system. Additionally, the adsorption capacity of SMS for different sulfas varied owing to differences in their chemical structures and functional groups.

Kinetic data describing adsorption fit the pseudo-second-order kinetic model well. Additionally, an intra-particle diffusion study showed that film diffusion was operating during the process of sulfas adsorption onto SMS. The equilibrium experimental data fit the Langmuir isotherm well, and the maximum adsorption capacity was 2.1072, 1.8103, 2.2991, and 2.2133 $\mathrm{mg\,g^{-1}}$ at 288 K for SM, SM2, ST, and SMX, respectively. Overall, these findings indicate that SMS is an effective adsorbent for the removal of trace concentrations of sulfas from aqueous solution. Therefore, we investigated use of this agricultural waste as a low-cost adsorbent to remove sulfas from water while reducing agricultural waste, thereby improving the environment.

Acknowledgments

The authors are grateful for a research grant provided by the China National Ministry of Science and Technology (Grant no. 2012BAJ25B00). We also thank the Key Laboratory of Groundwater Resources and Environment, Ministry of Education, Jilin University, and the Institute of Water Resources and Environment of China for helping us implement this project. Finally, we are grateful to the students who assisted us with this project and the anonymous reviewers of the manuscript.

References

[1] J. Gao, J.A. Pedersen, Adsorption of sulfonamide antimicrobial agents to clay minerals, Environ. Sci. Technol. 39 (2005) 9509–9516.

[2] R. Hirsch, T. Ternes, K. Haberer, K.L. Kratz, Occurrence of antibiotics in the aquatic environment, Sci. Total Environ. 225 (1999) 109–118.

[3] K. Berger, B. Petersen, H. Buening-Pfaue, Persistenz von Gülle-Arzneistoffen in der Nahrungskette (Persistence of medicaments from liquid manure in the food chain), Arch. Lebensmittelhyg 37 (1986) 85–108.

[4] D.W. Kolpin, E.T. Furlong, M.T. Meyer, E.M. Thurman, S.D. Zaugg, L.B. Barber, H.T. Buxton, Pharmaceuticals, hormones, and other organic wastewater contaminants in US Streams, 1999–2000: A national reconnaissance, Environ. Sci. Technol. 36 (2002) 1202–1211.

[5] K.G. Karthikeyan, M.T. Meyer, Occurrence of antibiotics in wastewater treatment facilities in Wisconsin, USA, Sci. Total. Environ. 361 (2006) 196–207.

[6] J.A. Pedersen, M.A. Soliman, I.H. Suffet, Human pharmaceuticals, hormones, and personal care product ingredients in runoff from agricultural fields irrigated with treated wastewater, J. Agric. Food Chem. 53 (2005) 1625–1632.

[7] C.A. Kinney, E.T. Furlong, J. Cahill, Occurrence and Behavior of Wastewater-Derived Pharmaceuticals in Soils Irrigated by Reclaimed Wastewater, American Chemical Society, Washington, DC, 2004.

[8] D. Zhang, L. Lin, Z. Luo, Occurrence of selected antibiotics in Jiulongjiang River in various seasons, South China, J. Environ. Monit. 13 (2011) 1953–1960.

[9] X.S. Miao, F. Bishay, M. Chen, Occurrence of antimicrobials in the final effluents of wastewater treatment plants in Canada, Environ. Sci. Technol. 38 (2004) 3533–3541.

[10] A.L. Batt, S.A. Diana, Simultaneous analysis of multiple classes of antibiotics by ion trap LC/MS/MS for assessing surface water and groundwater contamination, Analy. Chem. 77 (2005) 2940–2947.

[11] D.W. Kopli, E.T. Furlong, M.T. Meyer, Pharmaceuticals, hormones, and others organic wastewater contaminants in US streams, 1999–2000: A national reconnaissance, Environ. Sci. Technol. 36 (2002) 1202–1211.

[12] S. Managaki, A. Murata, H. Takada, Distribution of macrolides, sulfonamides, and trimethoprim in tropical waters: Ubiquitous occurrence of veterinary antibiotics in the Mekong Delta, Environ. Sci. Technol. 41 (2007) 8004–8010.

[13] A.B. Boxall, D.W. Kolpin, B. Halling-Sorensen, J. Tolls, Are veterinary medicines causing environmental risks? Environ. Sci. Technol. 37 (2003) 286A–294A.

[14] J.C. Chee-Sanford, R.I. Aminov, I.J. Krapac, N. Garrigues-Jeanjean, R.I. Mackie, Occurrence and diversity of tetracycline resistance genes in lagoons and groundwater underlying two swine production facilities, Appl. Environ. Microbiol. 67 (2001) 1494–1502.

[15] L. Wollenberger, B. Halling-Sørensen, K.O. Kusk, Acute and chronic toxicity of veterinary antibiotics to *Daphnia magna*, Chemosphere 40 (2000) 723–730.

[16] M.L. Richardson, J.M. Bowron, The fate of pharmaceutical chemicals in the aquatic environment, J. Pharm. Pharmacol. 37 (1985) 1–12.

[17] F.M. Christensen, Pharmaceuticals in the environment—A human risk? Regul. Toxicol. Pharmacol. 28 (1998) 212–221.

[18] S.F. Webb, A data-based perspective on the environmental risk assessment of human pharmaceuticals III: Indirect human exposure, in: K. Kümmerer (Ed.), Pharmaceuticals in the Environment, Springer-Verlag, Berlin, 1999, pp. 221–230.

[19] W.S. Kuo, R.W. Regan, Aerobic carbamate bioremediation aided by compost residuals from the mushroom industry: Laboratory studies, Compost. Sci. Util. 6 (1998) 19–29.

[20] M.D. Webb, G. Ewbank, J. Perkins, A.J. McCarthy, Metabolism of pentachlorophenol by *Saccharomonospora viridis* strains isolated from mushroom compost, Soil Biol. Biochem. 33 (2001) 1903–1914.

[21] M. Guo, J. Chorover, R. Rosario, Leachate chemistry of field-weathered spent mushroom substrate, J. Environ. Qual. 30 (2001) 1699–1709.

[22] S.W. Chiu, S.Ch. Law, M.L. Ching, K.W. Cheung, M.J. Chen, Themes for mushroom exploitation in the 21st century: Sustainability, waste management, and conservation, J. Gen. Appl. Microbiol. 46 (2000) 269–282.

[23] Z. Qiang, C. Adams, Potentiometric determination of acid dissociation constants (P_{Ka}) for human and veterinary antibiotics, Water Res. 38 (2004) 874–2890.

[24] C.E. Lin, C.C. Chang, W.C. Lin, Migration behavior and separation of sulfonamides in capillary zone electrophoresis III. Citrate buffer as a background electrolyte, J. Chromatogr. A 768 (1997) 105–112.

[25] R. Ding, K. Gong, Super-absorbent resin preparation utilizing spent mushroom substrates, J. Appl. Polym. Sci. 130 (2013) 1098–1103.

[26] S.T. Akar, A. Gorgulu, Z. Kaynak, Biosorption of Reactive Blue 49 dye under batch and continuous mode using a mixed biosorbent of macro-fungus *Agaricus bisporus* and *Thuja orientalis* cones, Chem. Eng. J. 148 (2009) 26–34.

[27] G. Bayramoğlu, G. Çelik, M.Y. Arica, Biosorption of Reactive Blue 4 dye by native and treated fungus *Phanerocheate chrysosporium*: Batch and continuous flow system studies, J. Hazard. Mater. 137 (2006) 1689–1697.

[28] Z. Liu, Y. Miao, Z. Wang, G. Yin, Synthesis and characterization of a novel super-absorbent based on chemically modified pulverized wheat straw and acrylic acid, Carbohydr. Polym. 77 (2009) 131–135.

[29] Z. Ma, Q. Li, Q. Yue, B.Y. Gao, X. Xu, Q. Zhong, Synthesis and characterization of a novel super-absorbent based on wheat straw, Bioresour. Technol. 102 (2011) 2853–2858.

[30] R. Liang, H. Yuan, G. Xi, Q. Zhou, Synthesis of wheat straw–g-poly(acrylic acid) superabsorbent composites and release of urea from it, Carbohydr. Polym. 77 (2009) 181–187.

[31] D. Zhang, B. Pan, H. Zhang, P. Ning, B.S. Xing, Contribution of different sulfamethoxazole species to their overall adsorption on functionalized carbon nanotubes, Environ. Sci. Technol. 44 (2010) 3806–3811.

[32] M.J. Prieto, D. Bacigalupe, O. Pardini, J.I. Amalvy, C. Venturini, M.J. Morilla, E.L. Romero, Nanomolar cationic dendrimeric sulfadiazine as potential antitoxoplasmic agent, Int. J. Pharm. 326 (2006) 160–168.

[33] I. Braschi, G. Gatti, G. Paul, C.E. Gessa, M. Cossi, L. Marchese, Sulfonamide antibiotics embedded in high silica zeolite y: A combined experimental and theoretical study of host−guest and guest−guest interactions, Langmuir 26 (2010) 9524–9532.

[34] J. Guo, L. Li, Y. Ti, J. Zhu, Synthesis and properties of a novel pH sensitive poly(N-vinyl-pyrrolidone-co-sulfadiazine) hydrogel, Express Polym. Lett. 1 (2007) 166–172.

[35] P. Guru, R.K. Gautam, M.P. Goutam, Synthesis, spectral and toxicological studies of complex Zn (II) with sulfadiazine, Chem. Pap. 58 (2004) 341–347.

[36] G. Lv, Z. Li, N. Hoeppner, L. Wu, L. Liao, Interactions between sulfa drug sulfadiazine and hydrophobic talc surfaces, Colloids Surf., A 446 (2014) 172–178.

[37] W. Lertpaitoonpan, S.K. Ong, T.B. Moorman, Effect of organic carbon and pH on soil sorption of sulfamethazine, Chemosphere 76 (2009) 558–564.

[38] S. Lagergren, About the theory of so-called adsorption of soluble substances, KungLiga Svenska Vetensk. Handl. 24 (1898) 1–39.

[39] Y.S. Ho, McKay, Pseudo-second order model for sorption processes, Process Biochem. 34 (1999) 451–465.

[40] W.J. Weber, J.C. Morriss, Kinetics of adsorption on carbon from solution, J. Sanit. Eng. Div. Am. Soc. Civ. Eng. 89 (1963) 31–60.

[41] W. Giger, A.C. Alder, E.M. Golet, H.P.E. Kohler, C.S. McArdell, E. Molnar, H. Siegrist, M.J.F. Suter, Occurrence and fate of antibiotics as trace contaminants in wastewaters, sewage sludges, and surface waters, CHIMIA Int. J. Chem. 57 (2003) 485–491.

[42] B.H. Hameed, A.A. Rahman, Removal of phenol from aqueous solutions by adsorption onto activated carbon prepared from biomass material, J. Hazard. Mater. 160 (2008) 576–581.

[43] S.-H. Lin, R.S. Juang, Adsorption of phenol and its derivatives from water using synthetic resins and low-cost natural adsorbents: A review, J. Environ. Manage. 90 (2009) 1336–1349.

[44] Y. Al-Degs, M.A.M. Khraisheh, S.J. Allen, Effect of carbon surface chemistry on the removal of reactive dyes from textile effluent, Water Res. 34 (2000) 927–935.

[45] Y. Önal, C. Akmil-Basar, C. Sarıcı-Özdemir, Elucidation of the naproxen sodium adsorption onto activated carbon prepared from waste apricot: Kinetic, equilibrium and thermodynamic characterization, J. Hazard. Mater. 148 (2007) 727–734.

[46] H. Liu, Y. Dong, H. Wang, Y. Liu, Adsorption behavior of ammonium by a bioadsorbent—Boston ivy leaf powder, J. Environ. Sci. 22 (2010) 1513–1518.

[47] J. Ding, S.Y. Zhao, Q. Zhao, L. Ding, Activated carbons modified by oxidation remove sulfadiazine from aqueous phase, J. Harbin Univ. Comm. (Natur. Sci. Edition) 30 (2014) 41–45 (in China).

[48] X.L. Bao, Z.M. Qiang, W.W. Ben, Adsorptive removal of sulfonamides from water by magnetic nanocomposite CoFeM48, Environ. Sci. 33 (2013) 401–408 (in China).

[49] L.C. Duan, F.H. Wang, Y.X. Ji, F.Zhang, B. Zhao G.X. Wang, Adsorption removal of sulphonamide by fly ash from thermal power plant, Chin. J. Environ. Eng. 8 (2014) 2231–2236 (in China).